Theoretical Studies of Metal Ion Selectivity.† 2. DFT Calculations of Complexation Energies of Selected Transition Metal Ions (Co^{2+}, Ni^{2+}, Cu^{2+}, Zn^{2+}, Cd^{2+}, and Hg^{2+}) in Metal-Binding Sites of Metalloproteins

Lubomír Rulíšek* and Zdeněk Havlas

Institute of Organic Chemistry and Biochemistry, Academy of Sciences of the Czech Republic, and Center for Complex Molecular Systems and Biomolecules, Flemigovo náměstí. 2, 166 10 Prague 6, Czech Republic

Received: October 25, 2001; In Final Form: January 25, 2002

To obtain a deeper understanding of metal ion selectivity exhibited by different sites in biomolecules, the interactions of selected transition metal (TM) ions with model functional groups are further studied. The hypothesis is proposed that complexation energies of TM ions in metal-binding sites of a general formula $[MX_n]^{2+}$ can be estimated from the interaction energies of these ions with model functional groups X_i's and the quantitative evaluation of the cooperative effect. This effect is defined as the nonadditive part of the substitution energy of two functional groups for two water molecules in an $[M(H_2O)_n]^{2+}$ complex (reference state) in comparison with the sum of the substitution energies of the respective monosubstitutions (defining the interaction energy of X_i). The model functional groups used for the evaluation of the cooperative effect are OH^-, H_2S, SH^-, HCHO, $HCOO^-$, NH_3, and CH_3NCH_2. Four coordination geometries (linear, tetrahedral, square planar, and octahedral), six transition metal ions (Co^{2+}, Ni^{2+}, Cu^{2+}, Zn^{2+}, Cd^{2+}, Hg^{2+}), and all combinations of the above functional groups are taken into account. To ascertain the plausibility of the hypothesis, complexation energies of TM ions in several model complexes $[MX_n]^{2+}$ are calculated and compared with their estimated values. It is shown that the consideration of the cooperative effect (i.e., the three-body $X_i \cdots M \cdots X_j$ interaction term) is both essential and sufficient to yield the estimates that deviate, on a relative scale, by less than 2% (5−15 kcal mol^{-1}) from the calculated values. Finally, it is shown that the estimated (calculated) complexation energies of TM ions in metal-binding sites of two metalloproteins, carbonic anhydrase and carboxypeptidase A, are in a very good agreement with the experimentally determined stability constants.

I. Introduction

The interactions of transition metal (TM) ions with biomolecules (metalloproteins, peptides, DNA, RNA molecules, etc.) represent one of the fundamental aspects exploited by living organisms in performing their essential tasks. The role of TM ions in the structure and function of these systems is indispensable, though often unknown at the atomic or electronic level. Hence, many experimental and theoretical studies have been carried out to elucidate the mechanisms of metalloenzyme action (including transition-state structures and proton and electron transfer),[1] structural aspects of metal-binding sites,[2] and the energetics of biocatalysis.[3] From a conceptual point of view, most of these studies deal with a single model system mimicking a real metal-binding site and derive its properties from an analysis of quantum chemical data.

On the other hand, there are numerous studies[4] dealing with the interactions of a series of ligands with TM ion(s) or a series of TM ions interacting with small ligand(s). Their goal is a better understanding of the differences in the chemical behavior of TM ions, though they may sometimes suffer from the limited size of the model system, which complicates the comparison with other than sophisticated gas-phase experimental data. However, we feel that because of the growth of computational power and improvements in quantum chemical methodology in recent years the gap between these two approaches has diminished; consequently, the accumulated experience should bring the theoretical calculations closer to biochemically relevant TM systems in near future. Recent advances in the field are well-documented in excellent reviews.[5,6]

One of the most important properties of bioinorganic systems is the relationship between molecular structure and energetics. Molecular structures can be efficiently studied by atomic resolution experimental techniques, but they do not provide any energy values. Thus, it is very tempting to complement bioinorganic experiments with energy evaluations, which can be presently achieved by state-of-the-art QM calculations that provide unique insights into the reaction energetics,[7] transition-state barriers,[8] stability of different conformers or isomers,[9] or preferred binding sites in biomolecules[10] and yield the estimates of more general concepts such as the reaction pathway and metal ion selectivity.

It is the latter phenomenon that is the subject of this series of articles. There are three factors that determine the specificity of a given metal-binding site for a particular TM ion:[11] the coordination geometry, the size of the preformed cavity in more complex ligands, and the affinity of functional groups participating in metal−ligand bonds for a specific TM ion. The first factor has been addressed recently[12] by a careful analysis of the experimental structures of metal-binding sites in metalloproteins and smaller molecule crystal structures, which enabled us to assign the preferred coordination geometries for each of the TM ions and to evaluate the abundance of amino acid (AA) side chains in the metal-binding sites of the metalloproteins. The

* Corresponding author. E-mail: lubos@uochb.cas.cz. Tel and Fax: +420-2-20183292.

† Part 1: *J. Am. Chem. Soc.* **2000**, *122*, 10428.

10.1021/jp013951n CCC: $22.00
Published on Web 03/20/2002

second factor can be derived either from the experimental bond distances (ionic radii of TM ions)[13] or from the quantum chemical calculations (equilibrium metal−ligand distances).

The third factor, and probably the most difficult one to address, is the different affinities of the particular ligand for different TM ions, which is often based on qualitative or semiquantitative theories or principles such as the HSAB (hard and soft acids and bases) principle of Parr and Pearson[14] and the Irving−Williams (IW) series of stability constants.[15] Nevertheless, we believe that a quantitative evaluation of the affinity is feasible only with accurate quantum chemical calculations on model systems, which is why a reliable computational scheme for the calculations of TM complexes containing metal−ligand bonds with ionic character has been proposed.[16] It has been tested both for the complexes with nondegenerate ground electronic states (both closed- and open-shell systems) and for the species with degenerate or quasi-degenerate ground states (such as $[CoX_6]^{2+}$ in octahedral coordination geometry).[17] In these studies, the DFT/B3LYP method has been shown to yield substitution (reaction) energies of 0.5 kcal mol^{-1} accuracy when compared to reference CCSD(T) calculations, but at least triple-ζ basis sets with polarization and diffuse functions on all atoms should be used.

Using this scheme, the interaction energies of AA side chains (capped with hydrogen atoms) with the selected TM ions (Co^{2+}, Ni^{2+}, Cu^{2+}, Zn^{2+}, Cd^{2+}, Hg^{2+}) have been calculated and published in the preceding article of the series.[18] Four coordination geometries (octahedral, tetrahedral, square planar, and linear) have been taken into account for each TM ion, and AA side chains have been classified according to their affinity and selectivity toward these TM ions. The interaction energies and the selectivity factors were calculated as the substitution energies of one water molecule in the coordination sphere of TM ions (cf. eq 2 below). Naturally, the question arises of how these interaction energies and affinities are modified upon the simultaneous replacement of two or more water molecules, that is, if certain combinations of AA side chains enhance the specificity of the particular site or diminish it.

Therefore, in the present study, we discuss the effects of the simultaneous binding of two and more AA side chains to a particular TM ion,which also provides additional important information about the calculated interaction energies and selectivity factors derived from monosubstituted $[M(H_2O)_{n-1}X]^{2+}$ species.[19] We postulate a hypothesis that knowledge of the interaction energies of functional groups representing AA side chains and estimates of the cooperative effect (nonadditivity of interaction energies upon the disubstitution) yield the relative affinities of general $[MX_n]^{2+}$ metal-binding sites to a high degree of accuracy (X_n is a combination of AA side chains in a particular coordination geometry).

Description of the Systems. The study consists of the following steps:

(i). Calculations of the equilibrium geometries and molecular energies of monosubstituted $[M(H_2O)_{n-1}X]^{2+}$ complexes in each coordination geometry. The obtained values are used for the definition of the interaction energies of individual functional groups with M (for X = AA side chain, these interaction energies have been published in the preceding article,[18] but because the functional groups used in this study are different (smaller), this step must be included).

(ii). Calculations of the equilibrium geometries and molecular energies of the disubstituted $[M(H_2O)_{n-2}XY]^{2+}$ complexes. The obtained values are used for the definition of the cooperative effect. This effect is defined as the difference between the interaction energies of X and Y groups when they are bound simultaneously to M and the interaction energies of X and Y.

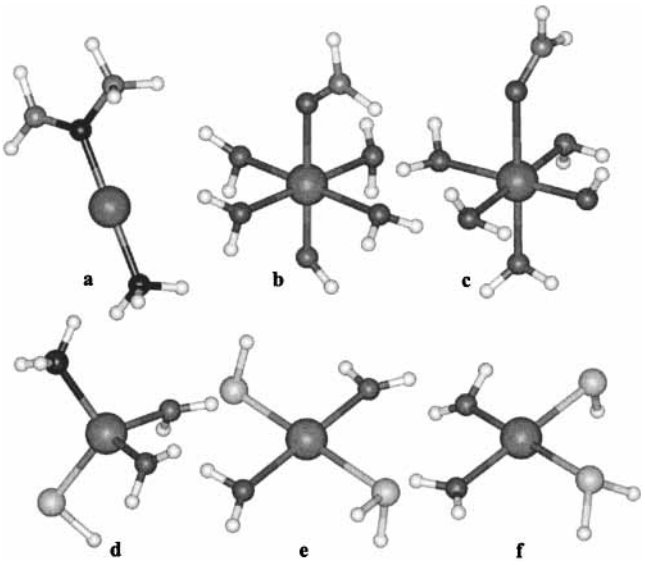

Figure 1. Structures of six representative complexes studied in this work: (a) $[M(NH_3)(CH_2NCH_3)]^{2+}$, **(b)** $[M(H_2O)_4(HCHO)(OH)]^{+}$, the trans isomer, **(c)** $[M(H_2O)_4(HCHO)(OH)]^{+}$, the cis isomer, **(d)** $[M(H_2O)_2(NH_3)(SH)]^{+}$, **(e)** $[M(H_2O)_2(H_2S)(SH)]^{+}$, the trans isomer, **(f)** $[M(H_2O)_2(H_2S)(SH)]^{+}$, the cis isomer.

(iii). Comparison of the stabilities of cis and trans isomers of square-planar and octahedral complexes.

(iv). Calculations of model "persubstituted" $[MX_n]^{2+}$ complexes with all water molecules in the reference complex $[M(H_2O)_n]^{2+}$ replaced with either AA side chains or simple groups representing them (to test the validity of the hypothesis formulated above).

(v). Comparison of the estimated (calculated) complexation energies with the experimentally determined stability constants for metal-binding sites of two metalloproteins − carbonic anhydrase and carboxypeptidase A.

The AA side chains are represented by seven model functional groups: H_2S (model for Met and protonated Cys), SH^- (deprotonated Cys), NH_3 (deprotonated Lys), HCHO (carbonyl oxygen of Asn, Gln, peptide bond oxygen, and protonated Asp, Glu), OH^- (deprotonated Ser, Thr, Tyr), $HCOO^-$ (deprotonated Asp, Glu), and CH_3NCH_2 (His). This choice is a compromise between three factors: (i) computational accuracy, (ii) selection of the functional groups representing AA side chains (ideally it should be whole side chains with hydrogens substituted for C_α carbons of the peptide backbone or with the NH_2CHCHO fragment as its model), and (iii) the number of combinations from the set of the selected functional groups (ideally, all combinations should be calculated, which amounts to $^1/_2n(n+1)$ systems for disubstituted complexes). We have decided to fulfill conditions (i) and (iii), that is, to achieve the high level of accuracy with B3LYP/6-311++(2df,2pd)//B3LYP/6-31+G(d) model chemistry and explore all the combinations of the model functional groups. Thus, we obtained 28 disubstituted complexes for each of six TM ions in each of six coordination arrangements (four coordination geometries and two isomers, cis and trans, in square-planar and octahedral coordination geometry), amounting to a total of 1008 systems.

In Figure 1, several representatives of the studied systems are depicted.

A note should be added about the broader perspective of this work and selection of the ions. TM ions studied in this work are both abundant in metal-binding sites of metalloproteins[20] and the major environmental pollutants (at least, in higher concentrations). This study characterizes the affinities of general mononuclear metal-binding sites,[21] which can be used, for example, for the molecular design of highly specific peptides[22] for efficient removal of these metals from the environment.

II. Computational Details

All the calculations were performed with the Gaussian 98 program suite[23] and in the framework of density functional theory (DFT). The three-parameter functional developed by Becke,[24] which combines the Becke gradient-corrected exchange functional and the Lee−Yang−Parr and Vosko−Wilk−Nusair correlation functionals[25] with part of the exact Hartree−Fock exchange energy, has been employed (denoted as B3LYP).

Two basis sets have been used throughout the calculations, denoted as BS1 and BS2. BS1 is the 6-31G basis set that is stored internally in Gaussian 98 both for the first- and second-row atoms and the first-row transition metals. BS1 was further augmented by diffuse functions: the (s, 2p, d) set for TMs, sp functions for other heavy elements and the single set of polarization functions, f for TMs, and d for other heavy elements.

BS2 consisted of the triple-ζ (TZ) basis set of Watchers and Hay[26] for the first-row transition metals (Co, Ni, Cu, Zn) and the standard 6-311G for other elements (H, C, N, O, S).[27] BS2 was augmented by the same diffuse functions as was BS1, with the further addition of s functions for hydrogens and the following sets of polarization functions: 2fg for TMs, 2df for other heavy atoms, 2pd for hydrogens. The exponents of all of the diffuse and polarization functions were used as implemented in Gaussian 98, and the described basis sets have been approached via 6-31+G(d) (BS1) and 6-311++G(2df, 2pd) (BS2) keywords.

For Cd^{2+} and Hg^{2+}, effective core potentials (ECP) of Stevens and co-workers[28] have been used (denoted SBKJ). To achieve consistency with the above-described basis sets used for the first-row TMs, the original valence basis set was further augmented with the following uncontracted GTO basis functions: diffuse d functions ($\alpha_d(Cd) = 0.075$, $\alpha_d(Hg) = 0.040$); f ($\alpha_f(Cd) = 0.775$, $\alpha_f(Hg) = 0.690$); and 2fg ($\alpha_{1f}(Cd) = 2.0$, $\alpha_{2f}(Cd) = 0.3$, $\alpha_g(Cd) = 0.775$, $\alpha_{1f}(Hg) = 1.35$, $\alpha_{2f}(Hg) = 0.35$, $\alpha_g(Hg) = 0.69$) sets of polarization functions, corresponding to BS1 and BS2, respectively.

The computational scheme consisted of several steps: First,-optimization of the molecular geometries of all Zn^{2+} complexes (both mono- and disubstituted species) have been carried out at the B3LYP/BS1 level, with the angles at the metal centers fixed to the values corresponding to the given coordination geometry and all other internal coordinates optimized.

Second, all other systems were assumed to adopt the geometry of the optimized Zn^{2+} complexes, and only n metal−ligand distances ($n = 2, 4, 6$) were optimized at the B3LYP/BS1 level. The only exceptions were octahedral Co^{2+} and Cu^{2+} complexes, which are, in principle, Jahn−Teller unstable as a consequence of the degenerate ground state in ideal O_h ligand-field symmetry. They have been assumed to adopt the same geometries as do the corresponding $[Ni(H_2O)_5X]^{2+}$ or $[Ni(H_2O)_4XY]^{2+}$ systems, with all six metal−ligand distances increased by the experimental and theoretical differences between the ionic radii of Co^{2+}, Cu^{2+}, and Ni^{2+} in octahedral coordination geometries that are +0.04 Å (Co^{2+}) and +0.03 Å (Cu^{2+}).[29] It is a plausible approximation and has been carefully tested in the previous work on model $[Co(H_2O)_5X]^{2+}$ complexes.[17] As for the usage of equilibrium geometries of Zn^{2+} complexes for other TM ions and by optimizing only the metal−ligand distances, it has been shown that it causes errors of less than 0.1 kcal mol^{-1} in the values of the interaction energies of simple ligands.[18]

Third, the single-point energy calculations of all of the studied structures have been carried out at the B3LYP/BS2 level to obtain the final molecular energies of $[M(H_2O)_{n-2}XY]^{2+}$ complexes.

Fourth, the metal ion at the optimized geometry has been replaced by the corresponding ghost atom Bq_M, and a single-point energy was calculated for $Bq_M(H_2O)_{n-2}XY$ systems.

A short note should be added about the described scheme. By introducing the coordination geometry constraints, we are fully aware that the optimized structure may not be necessarily the global minimum of the complex. However, we must stress that this constraint belongs to the chosen chemical model because the target structure represented by our model systems is the metalloprotein in the specific coordination geometry. Then, the ligands may be kept at the given coordination geometry by the structural constraints in the biomolecule that may prevent its collapsing into the minimum found for the small model systems.

Throughout this article, the interaction energy of functional groups X and Y binding simultaneously to the metal ion M in a given coordination geometry is defined as

$$E_{int}(M, X, Y) = E([M(H_2O)_{n-2}XY]^{2+}) - E(Bq_M(H_2O)_{n-2}XY) - (E([M(H_2O)_n]^{2+}) - E(Bq_M(H_2O)_n)), \quad (1)$$

where $n = 2$ (linear coordination geometry), 4 (square planar, tetrahedral), and 6 (octahedral). According to this equation, the computed interaction energy includes the correction for the nonbonding interactions between ligands and a part of the basis set superposition error (BSSE). For $Y = H_2O$ in eq 1, we obtain the interaction energy $E_{int}(M, X)$ of a single functional group X with M. On the other hand, replacing all water molecules with different functional groups (AA side chains), we obtain interaction energies of TM ions with persubstituted sites, denoted as $E_{int}(M, X_1,...,X_n)$.

$E_{int}(M, X)$ and $E_{int}(M, X, Y)$ are then used as the definition of a quantity central to this work, $\Delta E_{coop}(M, X, Y)$, which quantitatively describes the cooperative effect,

$$\Delta E_{coop}(M, X, Y) = E_{int}(M, X, Y) - (E_{int}(M, X) + E_{int}(M, Y)) \quad (2)$$

Dimensionless $p_{coop}(M, X, Y)$

$$p_{coop}(M, X, Y) = \Delta E_{coop}(M, X, Y)/(|E_{int}(M, X)| + |E_{int}(M, Y)|), \quad (2a)$$

quantifies the nonadditive part of the mainly electrostatic interaction between TM ions and ligands.

A note should be added about the spin multiplicities of complexes calculated in this work. Three of the TM ions, Zn^{2+}, Cd^{2+}, and Hg^{2+}, are d^{10} ions ; therefore, their complexes are closed-shell systems with singlet ground states. Cu^{2+} is a d^9 ion, and its complexes have the doublet ground state. As for Co^{2+} and Ni^{2+}, they were shown to have high-spin ground states in the types of complexes and coordination environments that are the subject of this work.[18] Therefore, all properties of Co^{2+}

TABLE 1: Interaction Energies, E_{int}(M, X), of Model Functional Groups with TM Ions Defined by Equation 1[a,b]

coordination geometry (CG)	TM\f.g.	H_2S	H_2CO	$HCOO^-$	CH_2NCH_3	NH_3	OH^-	SH^-
linear (Lin)	Co^{2+}	−12.6	−21.9	−295.2	−51.4	−33.1	−319.2	−291.6
	Ni^{2+}	−6.6	−13.8	−291.8	−45.5	−26.0	−318.9	−294.9
	Cu^{2+}	−21.5	−28.0	−309.7	−63.5	−38.9	−334.4	−324.0
	Zn^{2+}	−10.0	−10.0	−278.5	−45.2	−27.8	−306.9	−284.4
	Cd^{2+}	−12.1	−8.7	−266.6	−41.6	−26.4	−293.8	−277.7
	Hg^{2+}	−23.0	−9.7	−267.6	−53.6	−35.1	−306.3	−297.6
tetrahedral (TH)	Co^{2+}	5.3	−5.0	−221.3	−24.5	−16.6	−260.7	−227.7
	Ni^{2+}	2.5	−6.7	−225.9	−28.1	−18.9	−266.3	−235.4
	Cu^{2+}	−3.2	−9.1	−234.3	−35.6	−23.6	−275.5	−251.6
	Zn^{2+}	4.1	−4.2	−222.0	−24.7	−17.6	−257.8	−228.8
	Cd^{2+}	0.2	−4.1	−214.4	−23.5	−17.1	−249.5	−228.4
	Hg^{2+}	−8.3	−4.5	−221.0	−30.1	−22.0	−258.5	−247.4
square planar (SQ)	Co^{2+}	7.6	−6.6	−226.6	−23.6	−14.6	−251.4	−219.7
	Ni^{2+}	6.5	−4.2	−226.0	−25.7	−15.8	−261.8	−220.6
	Cu^{2+}	1.9	−4.5	−231.4	−29.9	−19.9	−255.6	−229.8
	Zn^{2+}	5.7	−4.8	−224.8	−24.0	−16.2	−251.9	−225.3
	Cd^{2+}	1.5	−4.1	−214.0	−22.5	−16.2	−243.8	−225.2
	Hg^{2+}	−8.4	−3.5	−218.9	−30.5	−23.7	−258.7	−248.5
octahedral (OH)	Co^{2+}	12.1	0.5	−191.1	−10.6	−10.0	−222.5	−191.3
	Ni^{2+}	9.9	−1.8	−196.0	−16.3	−12.7	−223.2	−195.1
	Cu^{2+}	6.2	−2.9	−199.5	−21.8	−17.6	−235.8	−207.3
	Zn^{2+}	11.5	−0.3	−191.9	−13.6	−10.6	−223.0	−192.3
	Cd^{2+}	7.5	−0.8	−186.1	−13.8	−11.0	−216.9	−193.4
	Hg^{2+}	1.8	−1.3	−191.2	−19.6	−15.3	−231.0	−214.7

[a] All values are in kcal mol^{-1}. [b] The smaller (more negative) values indicate the higher affinity of a substituting functional group for the TM ion (compared to that of H_2O)

and Ni^{2+} complexes were calculated for the quartet and triplet ground states, respectively.

III. Results and Discussion

The Cooperative Effect: Interaction Energies. The cooperative effect is defined (see eq 2) as the nonadditive part of the interaction energy of functional groups X and Y (i.e., the energy of substitution of two water molecules in perhydrated $[M(H_2O)_n]^{2+}$ complexes) with a given TM ion. Therefore, we have calculated the interaction energies of model functional groups (OH^-, H_2S, SH^-, HCHO, $HCOO^-$, NH_3, CH_3NCH_2) with the TM ions first. The results of these calculations are summarized in Table 1.

There is very good agreement between the published values of the interaction energies of whole AA side chains with the TM ions[18] and those of simple functional groups representing them in this work. Therefore, the discussion concerning the monosubstituted complexes and computed data in Table 1 is not repeated in this article.

Then, the interaction energies E_{int}(M, X, Y) were computed for all 1008 disubstituted species, and the values of ΔE_{coop}(M, X, Y), a key quantity of this work, were calculated according to eq 2. They are summarized in Table 2. Because of limited space and the minimum of 1008 numbers that must be presented, we decided not to include explicitly the values of E_{int}(M, X, Y) or p_{coop}(M, X, Y) in tabular form. Both of these quantities could be easily calculated from ΔE_{coop}(M, X, Y), E_{int}(M, X), and E_{int}(M, Y).

As can be seen in Table 2, there are noticeable trends in the values of ΔE_{coop}(M, X, Y), and they will be used as the starting point of the discussion.

(a) For neutral ligands and coordination geometries other than linear (i.e., for coordination numbers $n \geq 4$), the values of ΔE_{coop}(M, X, Y) are below 2 kcal mol^{-1} (see Table 2) for 205 out of 300 systems (68%), which means that the cooperative effect is rather small in these cases, implying that the specificities of metal-binding sites containing only *neutral* residues can be derived from the interaction energies of AA side chains with hydrated TM ions with reasonable accuracy.

(b) On the other hand, the values of ΔE_{coop}(M, X, Y) for anionic ligands and linear coordination geometry are (with a few exceptions) positive and of nonnegligible magnitudes, which means that the substitution of the second functional group for H_2O is less favorable than that of the first. It is a consequence of the fact that the second functional group does not compete for TM ions with n water molecules of the first coordination sphere but with $(n - 1)$ water molecules and the already-bound first functional group (whose binding is stronger than that of water, as can be judged from the negative values of the interaction energies of the functional groups listed in Table 1); therefore, the magnitude of its effective interaction lowers. This effect is most pronounced in linear coordination geometry and for the complexes containing two anionic functional groups. In the former case, the strength of interaction of a TM ion with a particular ligand (approximately equivalent to $^1/_n$, where n is the coordination number) plays a key role and makes all the substitution energies (and also cooperative effect) larger in comparison with those of other coordination geometries. In the latter case, it is caused by the fact that the interaction between a TM ion and an anionic ligand is higher, in vacuo, by an order of magnitude in comparison with that of the neutral ligands. Then, from the same reason as that discussed above, the binding of the second anionic ligand is less effective. The interatomic distance between the metal and the first ligand increases (electrostatic weakening) by 0.05−0.10 Å, and the charge transfer from the ligand to the metal decreases (covalent contribution). However, it should be remembered that although ΔE_{coop}(M, X, Y) is large in the case of two anionic groups, its relative value, p_{coop}(M, X, Y), is quite moderate, in most cases about 0.03 (3%). Still, the calculations suggest that the chemical behavior of the metal-binding sites containing negatively charged functional groups is less predictable from quantum chemical calculations performed for isolated systems. In this context, we remind the reader that there is some discussion in the literature[30] concerning the applicability of negatively charged ligands as models of deprotonated AA side chains. It has been pointed out that the effects in which negatively charged residues participate may differ considerably in vacuo, in protein environ-

TABLE 2: Calculated Changes in Interaction Energies[a] upon the Simultaneous Binding of Two Functional Groups X and Y, ΔE_{coop}(M, X, Y), Defined by Equation 2, in Four Coordination Geometries (All Values in kcal mol^{-1}).[b]

	linear						Th						SQ_Eq (trans)					
	Co^{2+}	Ni^{2+}	Cu^{2+}	Zn^{2+}	Cd^{2+}	Hg^{2+}	Co^{2+}	Ni^{2+}	Cu^{2+}	Zn^{2+}	Cd^{2+}	Hg^{2+}	Co^{2+}	Ni^{2+}	Cu^{2+}	Zn^{2+}	Cd^{2+}	Hg^{2+}
H_2S, H_2S	11.5	2.5	15.3	3.3	3.5	6.3	−0.6	0.4	4.1	−0.7	0.3	2.3	−1.5	−2.4	−0.4	0.3	1.9	8.7
H_2S, H_2CO	10.4	1.9	14.3	1.5	1.4	1.9	0.3	1.5	5.4	−0.1	0.3	0.3	0.4	−1.1	0.0	0.1	0.4	0.5
H_2S, Imi[c]	14.3	5.4	19.7	5.4	5.2	8.6	1.3	1.5	7.2	0.7	1.7	4.2	0.4	0.0	1.3	2.1	3.0	9.8
H_2S,NH	13.0	3.3	15.3	3.3	3.2	5.5	0.7	1.5	6.6	0.8	1.4	3.1	0.4	−0.3	1.9	2.1	3.3	10.4
H_2S, SH^-	19.4	12.8	25.4	15.2	15.0	21.0	3.4	5.6	9.0	4.6	6.2	11.5	−2.8	−2.9	2.2	2.0	4.2	12.6
H_2CO,H_2CO	11.8	3.7	20.4	2.9	3.3	6.4	0.8	3.3	4.0	0.4	0.5	−0.1	1.3	−0.9	−0.5	1.0	0.6	−0.1
H_2CO, Imi	13.4	10.0	22.8	4.0	4.2	7.2	0.5	2.5	5.8	0.4	0.7	0.8	3.2	1.6	2.6	1.6	1.1	−0.5
Imi, Imi	18.7	10.4	26.9	7.4	7.0	10.8	2.9	4.3	13.0	2.9	3.7	6.4	5.1	4.2	5.8	5.4	5.5	12.6
NH_3,H_2CO	11.5	2.5	14.4	1.3	1.3	1.9	0.9	2.0	4.9	0.3	0.5	0.5	1.6	0.2	1.7	0.5	0.6	0.9
NH_3, Imi	14.1	7.7	17.2	3.8	3.7	6.1	2.0	2.2	8.0	1.9	2.5	4.4	2.2	1.1	2.4	3.6	4.1	11.3
NH_3, NH_3	13.0	2.6	13.1	2.0	2.0	3.4	1.4	1.1	6.4	1.3	1.8	3.2	1.1	−0.1	1.9	3.0	4.1	11.8
OH^-, H_2S	20.0	13.8	25.8	14.5	13.8	18.4	4.1	6.3	12.1	5.2	5.9	9.6	−8.1	−1.5	−3.4	−2.9	−1.2	7.2
OH^-, H_2CO	18.9	10.8	29.9	7.8	7.0	7.2	4.5	8.3	10.5	4.5	4.9	5.3	−1.7	3.8	−3.6	−0.2	0.1	0.3
OH^-, Imi	28.9	22.6	40.3	18.0	17.6	23.2	10.8	17.0	24.0	10.9	11.0	14.9	4.6	12.3	8.0	9.6	9.3	19.0
OH^-, NH_3	16.1	8.2	19.7	7.2	7.8	11.2	1.8	6.4	10.0	1.7	2.8	5.6	−8.7	−1.8	−4.3	−3.4	−1.5	8.2
OH^-, OH^-	45.6	42.9	63.7	25.8	29.2	37.7	35.5	34.0	43.0	22.6	23.5	30.0	15.5	33.0	14.3	22.0	21.3	40.4
OH^-, SH^-	61.0	61.9	89.2	41.3	43.3	54.8	34.7	39.9	55.0	28.6	30.1	38.7	17.1	20.9	16.3	26.8	28.1	50.5
SH^-, H_2CO	19.3	11.7	26.1	7.8	7.0	7.9	4.0	6.0	10.5	4.3	4.6	5.2	−4.4	−10.6	−5.4	−1.0	−1.0	−1.4
SH^-, Imi	31.2	25.4	43.7	21.1	20.8	28.3	9.7	12.6	24.2	9.8	10.9	16.5	−0.8	−5.3	4.5	6.7	7.3	16.8
SH^-, NH_3	17.8	10.3	22.2	9.8	10.4	15.3	2.6	3.6	11.5	2.9	4.2	8.5	−4.5	−7.1	−0.3	3.1	4.6	13.6
SH^-, SH^-	73.1	77.1	111.9	54.2	55.8	69.7	40.9	53.9	59.2	34.0	37.2	50.6	17.5	12.8	20.9	30.9	35.0	60.0
$HCOO^-$, $HCOO^-$	56.0	52.7	67.5	39.2	38.1	41.4	21.9	26.7	38.4	22.0	21.7	28.3	18.3	11.8	28.5	15.8	10.1	18.0
$HCOO^-$, Imi	31.9	24.3	40.9	21.1	19.7	24.9	9.5	11.5	22.9	10.1	10.1	14.3	−0.7	−6.1	14.1	1.2	−2.6	5.5
$HCOO^-$, H_2S	21.6	13.7	27.3	15.4	14.4	17.8	4.2	6.5	11.4	5.0	5.6	9.1	3.2	3.0	7.0	4.4	5.4	12.0
$HCOO^-$, HCHO	22.5	15.2	27.5	10.7	8.8	8.6	3.5	5.5	8.3	3.7	3.7	4.0	−6.3	−14.8	2.9	−6.3	−10.5	−9.4
$HCOO^-$, NH_3	30.2	10.8	20.6	9.0	9.0	12.2	3.0	4.7	10.7	3.3	3.8	6.6	0.3	0.1	2.5	0.8	2.5	9.6
$HCOO^-$, OH^-	59.6	48.1	80.0	33.1	33.3	38.2	21.3	24.3	34.9	19.5	19.0	25.1	14.1	17.3	14.7	14.7	17.3	24.0
$HCOO^-$, SH^-	67.0	62.1	100.2	47.2	46.5	52.6	26.7	30.6	42.8	26.0	26.6	35.0	18.0	11.8	21.8	21.7	22.4	32.7

	SQ_Anti (trans)						OH_Eq (cis)						OH_Anti (trans)					
	Co^{2+}	Ni^{2+}	Cu^{2+}	Zn^{2+}	Cd^{2+}	Hg^{2+}	Co^{2+}	Ni^{2+}	Cu^{2+}	Zn^{2+}	Cd^{2+}	Hg^{2+}	Co^{2+}	Ni^{2+}	Cu^{2+}	Zn^{2+}	Cd^{2+}	Hg^{2+}
H_2S, H_2S	−1.0	−1.0	1.5	−0.4	0.1	0.8	−2.2	−0.5	0.8	−0.8	0.2	2.0	−1.9	0.2	1.2	−0.4	−0.3	−1.7
H_2S, H_2CO	−0.5	−0.8	1.1	0.8	1.2	2.7	−2.8	0.0	1.7	−0.4	0.2	0.1	−2.4	0.5	1.0	−0.2	0.2	−0.1
H_2S, Imi[c]	0.7	0.5	4.0	0.4	0.9	1.2	−4.1	0.4	2.4	−0.2	0.7	3.3	−3.1	0.9	2.5	−0.3	−0.1	−2.6
H_2S, NH_3	−0.4	0.1	2.6	0.1	0.4	0.5	2.8	0.8	2.9	0.1	1.1	3.4	5.8	0.8	4.7	−0.3	−0.2	−2.6
H_2S, SH^-	0.5	1.9	6.4	2.8	3.5	7.1	1.6	4.3	5.1	1.2	2.9	6.6	1.7	1.9	1.3	−2.0	−2.3	−5.0
H_2CO, H_2CO	0.1	0.9	0.1	0.8	0.6	0.2	−2.9	0.8	1.0	−0.2	0.2	0.4	−0.9	0.7	1.5	0.6	1.0	0.6
H_2CO, Imi	1.3	0.4	1.1	0.9	0.7	0.1	−4.2	1.1	0.8	−0.6	−0.5	−0.4	−4.4	1.3	2.9	0.1	0.2	1.3
Imi, Imi	2.6	3.4	5.2	0.6	0.4	−2.1	−4.9	2.2	7.4	1.9	2.5	6.9	−5.5	2.1	4.0	−0.3	−0.1	−4.0
NH_3, H_2CO	−0.3	−0.3	0.7	1.0	1.1	1.6	−2.5	0.4	1.6	−0.5	0.0	0.1	−1.8	1.0	1.3	0.3	0.7	0.1
NH_3, Imi	1.4	1.2	4.2	0.2	0.7	−0.3	2.4	1.9	5.9	1.6	2.1	5.3	−0.7	2.1	3.3	−0.2	0.0	−4.0
NH_3, NH_3	−0.5	0.3	2.3	0.0	0.1	−0.8	3.0	1.3	5.9	1.1	1.7	4.7	3.9	1.6	1.7	−0.5	−0.4	−4.3
OH^-, H_2S	−7.8	−1.5	−3.5	−5.4	−4.7	−2.5	−3.7	−1.0	0.8	−3.5	−1.5	3.7	2.3	3.0	5.8	1.4	1.3	−1.1
OH^-, H_2CO	2.6	11.7	0.4	1.9	1.2	0.8	5.8	7.0	9.5	6.4	6.3	7.3	1.0	2.4	4.2	1.7	2.0	2.4
OH^-, Imi	−0.1	8.6	4.7	−1.0	−1.1	−1.7	6.1	10.1	16.3	10.0	10.3	17.8	2.5	7.4	10.6	2.8	2.8	−1.1
OH^-, NH_3	−9.2	−3.1	−5.7	−9.2	−7.9	−7.7	3.9	5.4	12.1	5.7	6.8	14.4	2.5	4.8	6.1	−0.7	−0.3	−4.9
OH^-, OH^-	0.7	14.9	6.3	−4.2	−1.4	2.6	38.9	35.7	51.0	36.6	35.1	50.8	27.4	25.2	32.7	13.3	13.1	10.0
OH^-, SH^-	7.0	11.1	14.3	3.6	6.8	15.7	34.3	33.9	49.4	33.1	32.8	49.0	25.7	26.2	35.0	14.8	14.9	15.0
SH^-, H_2CO	2.7	0.5	0.5	2.8	2.1	1.6	0.9	3.0	2.6	1.1	1.1	0.2	0.3	2.9	3.4	1.6	2.0	1.4
SH^-, Imi	6.4	8.8	12.4	5.1	5.0	6.9	2.4	7.0	11.1	6.2	6.8	13.3	1.7	7.3	8.6	0.4	0.3	−2.5
SH^-, NH_3	2.1	3.7	7.4	1.2	2.2	4.4	2.1	3.5	5.3	2.2	3.2	8.1	1.5	4.3	3.5	−3.4	−3.2	−6.8
SH^-, SH^-	9.4	4.0	20.0	9.0	13.6	26.5	30.4	30.2	42.7	30.6	32.8	52.7	25.6	25.0	33.3	13.0	13.4	17.8
$HCOO^-$, $HCOO^-$	12.4	6.4	22.7	10.0	4.0	8.2	11.5	14.7	20.6	12.3	12.5	18.7	7.2	10.9	13.5	7.0	7.3	7.9
$HCOO^-$, Imi	−2.5	−7.6	10.7	−3.3	−7.9	−4.7	0.0	4.8	8.6	3.1	3.3	8.0	1.2	7.1	8.5	4.2	4.0	1.1
$HCOO^-$, H_2S	5.0	5.1	9.5	5.6	5.2	6.5	−1.3	0.8	2.8	−0.3	1.5	4.8	1.6	4.1	6.2	2.4	2.5	1.0
$HCOO^-$, HCHO	−6.2	−14.2	2.5	−6.6	−11.2	−10.9	−2.5	−0.1	1.4	−1.0	−0.7	0.1	−2.9	0.0	−0.5	−1.1	−0.7	−0.9
$HCOO^-$, NH_3	5.0	5.5	8.2	4.2	3.6	2.5	−2.6	−0.2	3.2	−1.8	−1.0	2.8	0.7	3.8	4.4	1.0	1.2	−1.8
$HCOO^-$, OH^-	10.5	15.3	13.1	7.6	6.6	7.3	15.7	18.1	24.8	19.0	17.6	26.6	14.0	16.5	20.3	10.7	9.7	7.2
$HCOO^-$, SH^-	18.6	14.4	24.8	19.1	18.2	22.2	18.3	20.1	25.8	19.7	19.9	29.5	15.7	18.6	23.3	12.6	12.0	11.7

[a] The negative (positive) values indicate the enhanced (diminished) affinity of disubstituted site for a particular TM ion (compared with the coordination in the monosubstituted site). [b] For octahedral and square-planar coordination, both cis and trans isomers are calculated. [c] Imi = $CH_3N{=}CH_2$.

ments, and in water. Although the results we present seem to support this notion, we believe that their usage as models of deprotonated AA residues is fully justified and possibly more appropriate in (and only in) the comparative studies concerning the series of identically charged TM ions, as is done in this work.

TABLE 3: Comparison of Stability of Cis and Trans Isomers of $[M(H_2O)_{n-2}XY]^{2+}$ Complexes in Square-Planar (SQ) and Octahedral (OH) Coordination Geometries, Defined as $\Delta E_{cis-trans} = E([M(H_2O)_{n-2}XY]^{2+})_{cis} - E([M(H_2O)_{n-2}XY]^{2+})_{trans}$[a]

	SQ						OH					
	Co^{2+}	Ni^{2+}	Cu^{2+}	Zn^{2+}	Cd^{2+}	Hg^{2+}	Co^{2+}	Ni^{2+}	Cu^{2+}	Zn^{2+}	Cd^{2+}	Hg^{2+}
H_2S, H_2S	0.2	−0.4	−1.1	2.0	3.0	9.4	−0.1	−0.5	−0.1	−0.2	0.6	4.6
H_2S, H_2CO	0.4	−0.7	−1.4	−1.4	−1.3	−3.2	−0.8	−1.0	0.3	−0.7	−0.5	−0.2
H_2S, Imi	−0.1	−0.3	−2.3	1.9	2.2	8.9	−1.0	−0.5	0.0	0.3	1.0	6.8
H_2S, NH_3	0.2	−0.6	−1.3	2.5	3.4	11.0	−0.2	−0.6	1.1	0.2	1.1	6.8
H_2S, SH^-	0.0	−1.3	−0.7	2.2	3.6	8.0	−3.4	−0.8	0.6	0.2	2.3	8.8
H_2CO, H_2CO	0.8	−2.2	−1.2	0.1	−0.2	−0.3	0.2	1.1	1.8	0.3	0.2	0.9
H_2CO, Imi	1.8	1.2	1.4	0.5	0.2	−1.3	0.5	0.0	−1.9	−0.6	−0.3	−1.7
Imi, Imi	3.0	1.4	1.6	5.6	5.0	14.9	0.8	0.3	3.6	2.3	2.8	11.8
NH_3, H_2CO	1.1	0.0	0.4	−1.3	−0.9	−1.3	−0.8	−0.8	0.2	−0.8	−0.6	0.0
NH_3, Imi	0.7	0.2	−1.4	3.8	3.4	12.0	3.1	−0.2	2.7	2.0	2.3	10.2
NH_3, NH_3	1.6	0.3	0.2	4.7	4.8	14.1	−0.2	0.4	4.9	3.0	2.7	10.8
OH^-, H_2S	−1.4	−1.3	−1.7	2.0	2.5	9.2	−0.5	1.6	0.5	1.2	2.1	9.5
OH^-, H_2CO	−3.1	−5.8	−2.2	−1.3	−1.5	−1.1	0.2	−0.3	0.7	0.3	0.7	1.6
OH^-, Imi	2.1	0.9	−0.1	8.1	8.5	19.4	1.7	0.7	3.8	5.0	5.5	16.7
OH^-, NH_3	0.2	0.9	0.5	5.9	5.8	15.6	0.5	−0.2	5.1	5.5	5.7	17.5
OH^-, OH^-	11.8	14.7	3.8	22.6	22.1	35.9	2.7	1.5	9.4	10.8	12.5	29.0
OH^-, SH^-	8.5	8.0	−0.4	20.7	21.4	34.3	5.1	4.3	10.9	12.0	12.7	27.1
SH^-, H_2CO	−2.3	−5.4	−0.5	−0.2	−0.3	−1.1	2.0	1.3	0.6	0.8	0.6	0.4
SH^-, Imi	0.6	−5.5	−0.1	8.3	8.1	14.4	0.7	−0.2	2.6	5.5	6.0	15.3
SH^-, NH_3	0.3	−3.1	−0.9	8.0	7.4	13.4	0.5	−0.7	1.7	6.0	6.1	14.6
SH^-, SH^-	9.2	9.5	1.3	21.4	21.9	33.4	−1.0	−0.5	3.7	9.2	12.0	26.7
$HCOO^-$, $HCOO^-$	2.6	2.2	2.3	2.2	3.3	6.5	3.2	2.5	5.9	3.5	4.2	8.4
$HCOO^-$, Imi	0.7	0.5	1.9	3.2	3.1	7.7	2.1	1.2	3.5	2.0	1.9	8.1
$HCOO^-$, H_2S	−0.9	−0.9	−1.5	−0.6	−0.2	4.1	0.2	0.0	−0.2	0.4	1.4	5.3
$HCOO^-$, HCHO	−1.2	−1.7	−0.7	−0.8	−0.7	0.1	−0.2	−0.7	1.3	−0.4	−0.4	0.6
$HCOO^-$, NH_3	−0.6	−1.4	−1.7	0.2	1.5	8.5	0.5	−0.1	2.5	0.9	0.9	6.7
$HCOO^-$, OH^-	1.5	0.1	2.5	4.5	6.8	14.1	4.9	4.8	7.6	9.5	10.9	20.0
$HCOO^-$, SH^-	4.9	3.0	2.5	6.9	8.3	13.3	8.6	7.8	8.7	11.5	12.7	20.6

[a] The negative (positive) values (kcal mol^{-1}) indicate the higher stability of the cis (trans) isomer.

(c) The positive values of ΔE_{coop}(M,X,Y) are highest (on average) for Cu^{2+} and are followed by those for Hg^{2+}. This effect is most pronounced in linear coordination geometry (with a maximum of ΔE_{coop}(M, X, Y) = 111.9 kcal mol^{-1} for $[Cu(SH)_2]$). It indicates that the cooperative effect tends to modify the overestimated differences in the interaction energies, E_{int}(M, X), of single functional groups with the TM ions, which have been shown to correlate with the IW series of stability constants.[18] For example, the average interaction energies, $\bar{E}_{int}$(M, X), over all amino AA side chains in linear coordination geometry are −212.4 and −169.2 kcal mol^{-1} for Cu^{2+} and Zn^{2+}, respectively. However, because of the approximately two-fold larger cooperative effect exhibited by Cu^{2+} in this geometry, the difference in the interaction energies of two "average" AA side chains, $\bar{E}_{int}$(M, AA_1, AA_2), will be substantially less than 2 × 43.2 kcal mol^{-1} (∼86 kcal mol^{-1}); in fact, they will probably remain at the former value. For the qualitative explanation of this modification of the IW series, the same reasoning as above can be applied: the stronger bonding of the functional groups to TM ions (Cu^{2+} > Hg^{2+} >...) induces the larger cooperative effect.

(d) There are quite remarkable differences in the magnitude of the cooperative effect for cis and trans isomers of Hg^{2+}. This phenomenon will be explained in the section concerning the stability of cis and trans isomers of the complexes with square-planar and octahedral coordination geometries.

(e) Seven functional groups representing AA side chains can be classified according to their susceptibility to the cooperative effect as well. If we define $\Delta\bar{E}_{coop}$(Y) as the average of ΔE_{coop}(M, X, Y) over all six coordination arrangements, six TM ions, and seven functional groups X, then we obtain $\Delta\bar{E}_{coop}$(Y) = 4.3, 3.6, 7.0, 4.0, 14.4, 16.1, and 18.1 kcal mol^{-1} for H_2S, HCHO, CH_3NCH_2, NH_3, $HCOO^-$, OH^-, and SH^-, respectively. According to these average absolute values of ΔE_{coop}(M, X, Y), the cooperative effect is lowest for formaldehyde as the model for the carbonyl oxygen in AA side chains, followed by H_2S, NH_3, CH_3NCH_2, and the anionic residues $HCOO^-$, OH^-, and SH^- in the order given. However, this order may change if the relative scale is employed (i.e., if the above values are divided by the average interaction energy of each functional group that can be obtained from Table 1); therefore, this information is qualitative.

Because of the enormous number of studied systems, it is virtually impossible to explain all of the calculated values of ΔE_{coop}(M, X, Y) at the electronic level. Besides, in most cases, the differences in interaction energies are too small to prevent any meaningful analysis based upon the changes in electron densities accompanying the charge transfer from the ligands to metal, the polarizabilities of the ligands, etc. Neither can we think of any equation that would account for the computed values in a simple, concise form. In the context of this article, the numbers (values of ΔE_{coop}(M, X, Y)) themselves are of utmost importance because they represent three-body terms in the interaction energies of TM ions in a general metal-binding site, E_{int}(M, X_1,...,X_n), and enable us to estimate the specificity of a general $[MX_n]^{2+}$ site for the TM ions, as will be shown below. In the next subsection dealing with the stability of cis and trans isomers, we present an example of the analysis of the electronic distribution in complexes with ionic character that helps to explain some of the observed trends.

Comparison of the Stability of Cis and Trans Isomers. Because both the cis (equatorial) and trans (antipodal) isomers of disubstituted complexes were calculated in square-planar and octahedral coordination geometries, their molecular energies can be directly compared, and trends in their thermodynamic stability can be established. The values of $\Delta E_{cis-trans}$, defined simply as $\Delta E_{cis-trans}$(M, X, Y) = $E([M(H_2O)_{n-2}XY]^{2+})_{cis}$ − $E([M(H_2O)_{n-2}XY]^{2+})_{trans}$, are summarized in Table 3.

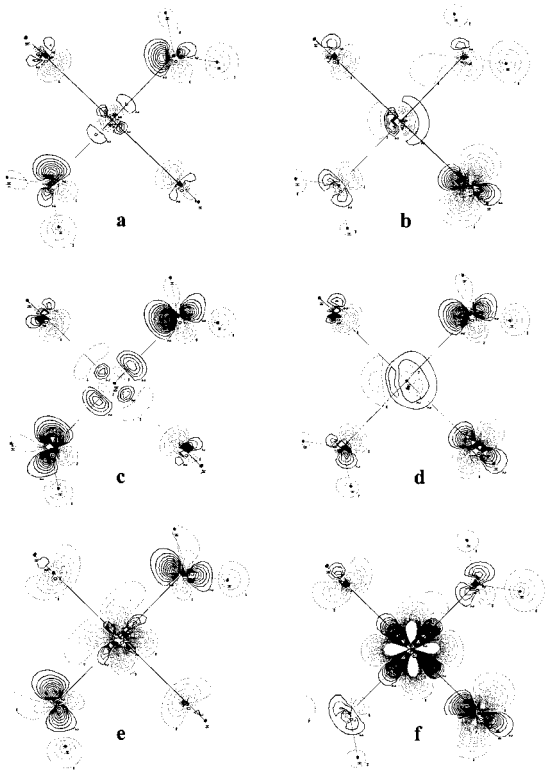

Figure 2. Differential maps of total electron densities, $\rho_{diff} = \rho([M(H_2O)_2(OH^-)_2]) - \rho(Bq(H_2O)_2(OH^-)_2) - (\rho([M(H_2O)_4]^{2+}) - \rho(Bq(H_2O)_4))$, of six complexes in square-planar coordination geometry: **(a)** M = Zn, trans, **(b)** M = Zn, cis, **(c)** M = Hg, trans, **(d)** M = Hg, cis, **(e)** M = Cu, trans, **(f)** M = Cu, cis.

As can be seen, $\Delta E_{cis-trans}$ is in most cases below 2 kcal mol^{-1}, which implies that both isomers have approximately equal stability. Still, there are several noticeable trends and exceptions.

(a) The first effect that can be observed in almost all systems is the higher stability of the trans isomers of charged ligands (OH^-, $HCOO^-$, SH^-) and to a lesser extent, of CH_3NCH_2 (which is the strongest Lewis base from neutral ligands). We presumed that this effect could be explained on the basis of purely electrostatic repulsion between the charged ligands, which is approximately 1.4 times higher in the cis position. However, the situation is quite different. Whereas $\Delta E_{cis-trans}$ is about 20 kcal mol^{-1} for charged ligands in square-planar coordination and 10 kcal mol^{-1} for those in octahedral coordination, the $\Delta E^{lig}_{cis-trans}$ value for ligands without a TM ion is considerably below 10 kcal mol^{-1} in square-planar coordination. For example, $\Delta E^{lig}_{cis-trans}(Bq_{Zn}, OH^-, OH^-) = 4.2$ kcal mol^{-1} at the B3LYP/BS2 level or 3.6 kcal mol^{-1} at the MP2/BS2 level. When looking for alternative explanations, the differential maps of the $[Zn(H_2O)_2(OH)_2]$ complex in cis and trans configurations were analyzed and compared with the reference $[Zn(H_2O)_4]^{2+}$ complex. As can be seen in Figure 2a and b, there is considerable charge transfer from two OH^- groups, which causes an increase in the electron density along the $Zn-OH^-$ bonds (and a decrease in the electron density along the remaining two $Zn-OH_2$ bonds), with its maximum approximately 0.2 Å from zinc. It is obvious that this charge transfer is more effective for the trans configuration and causes the lowering of molecular energy of the trans complexes with two negatively charged functional groups with respect to the cis isomers.

(b) In both square-planar and octahedral coordination geometries, the higher stability of the trans isomers of Hg^{2+} complexes (with the exception of the H_2CO ligand that slightly prefers the cis position with respect to all six ligands) can be observed. Qualitatively, this stability can be explained by the tendency of mercury(II) to prefer linear coordination geometry.[12,13,18] To provide a more rigorous explanation, the same analysis as that for zinc(II) systems has been performed. As can be seen in Figure 2c and d, there is the analogous charge transfer from ligands to metal as described above, but it is much higher for the *trans*-$[Hg(H_2O)_2(OH)_2]$ complex (in comparison with the equivalent zinc(II) system) and approximately the same for the cis isomers of Zn^{2+} and Hg^{2+}. It effectuates further lowering of the molecular energy of the trans isomer and the increase in the value of $\Delta E_{cis-trans}$.

(c) The exceptions to the trends described above are copper(II) complexes in square-planar coordination geometry. The $\Delta E_{cis-trans}$ value is close to zero, even for species with two negatively charged ligands. Again, this fact can be explained on the basis of charge transfer. The differential maps of electron density for $[Cu(H_2O)_2(OH)_2]$ complexes are depicted in Figure 2e and f. Whereas for closed-shell d^{10} systems the charge transfer is along the M−O bonds, for copper(II) molecules, the electrons of the ligands can be accommodated in partially filled d orbitals. Thus, a resulting map of electron density becomes symmetric, and the energies of the cis and trans isomers of Cu^{2+} square-planar systems are equal.

We believe that these analyses help us to understand some of the observed trends and illustrate the possibilities of how these effects can be explained at the electronic level (as has been mentioned in the previous subsection). However, similar analyses can be successfully employed only if the energy differences accompanying the processes are relatively large, at least 10 kcal mol^{-1}.

Persubstituted $[MX_n]^{2+}$ Complexes as Realistic Models of Metal-Binding Sites. So far, we have calculated the interaction energies of AA side chains with TM ions and the changes in these energies when the second functional group replaces a water molecule from the first coordination shell of a TM ion. In all coordination geometries, the reference state is the perhydrated complex $[M(H_2O)_n]^{2+}$ (n= 2, 4, 6), and the interaction energy is defined as the energy of substitution of the respective number of water molecules. It is almost impossible to carry these model calculations further, that is, to calculate all combinations of tri- and tetra- (for tetrahedral, square-planar, and octahedral geometry), or even penta- and hexa- (for octahedral geometry) substituted complexes with today's computational power. For example, the number of chemically distinct trisubstituted complexes $[M(H_2O)_3XYZ]^{2+}$ for a single TM ion in octahedral coordination geometry (and for the set of seven functional groups that is used in this work) would amount to 280 (cf. 56 for disubstituted species). Therefore, it remains for us to demonstrate how quantitative knowledge of the cooperative effect significantly improves the estimated values of $E_{int}(M, X_1,...,X_n)$, that is, the relative affinities of the studied TM ions toward a persubstituted metal-binding site. This demonstration is done in two steps.

In the first step, the calculations of $E_{int}(M, X_1,...,X_n)$ were carried out for seven model $[MX_n]^{2+}$ complexes (three in tetrahedral, three in square-planar, and one in octahedral coordination geometry), in which all X_i ligands belong to the set of seven functional groups studied in this work. The same computational scheme was used again. The only exception was that the systems were not assumed to adopt the geometry of zinc(II) complexes (with the subsequent partial optimization of only n metal−ligand distances), but all internal degrees of freedom other than the angles at the metal center (fixed at the

TABLE 4: Calculated Interaction Energies, E_{int}(M, X_1,..., X_n, calcd), of Persubstituted Sites Containing Ligands X_1,..., X_n with TM Ions, Defined by Equation 1, Compared with Their Estimated Values, E_{int}(M, X_1,..., X_n, est), Defined by Equation 3[a]

CG[b]	ligands	interaction energy	Co^{2+}	Ni^{2+}	Cu^{2+}	Zn^{2+}	Cd^{2+}	Hg^{2+}
TH	HCHO, NH_3, OH^-, SH^-	E_{int}(calcd)	−472.6	−481.9	−492.2	−472.4	−460.9	−478.3
		$\Sigma E_{int}(X_i)$	−510.0	−527.3	−559.9	−508.2	−499.2	−532.4
		E_{int}(est)	−485.8	−494.2	−508.7	−487.1	−475.6	−500.5
		ΔE(calc−est)	13.2	12.3	16.5	14.7	14.7	22.2
	HCHO, NH_3, SH^-, H_2S	E_{int}(calcd)	−235.5	−245.5	−264.0	−232.4	−232.1	−254.2
		$\Sigma E_{int}(X_i)$	−244.0	−258.5	−287.6	−246.3	−249.5	−282.2
		E_{int}(est)	−238.1	−248.3	−263.6	−239.9	−240.8	−267.7
		ΔE(calcd−est)	2.6	2.8	−0.4	7.5	8.7	13.5
	Imi, H_2O, OH^-, SH^-	E_{int}(calcd)	−470.0	−477.9	−490.5	−466.5	−458.4	−475.9
		$\Sigma E_{int}(X_i)$	−512.9	−529.8	−562.6	−511.3	−501.5	−535.9
		E_{int}(est)	−485.3	−495.0	−511.0	−486.7	−475.5	−500.9
		ΔE(calcd−est)	15.3	17.1	20.5	20.2	17.1	25.0
SQ	H_2S, NH_3, Imi, OH^-	E_{int}(calcd)	−273.8	−279.9	−286.2	−271.4	−262.0	−285.6
		$\Sigma E_{int}(X_i)$	−282.0	−296.8	−303.5	−286.4	−281.0	−321.2
		E_{int}(est)	−289.4	−293.6	−301.8	−287.1	−279.2	−303.6
		ΔE(calcd−est)	15.6	13.7	15.6	15.7	17.2	18.0
	H_2S, NH_3, OH^-, OH^-	E_{int}(calcd)	−503.3	−509.7	−505.8	−503.3	−487.1	−511.3
		$\Sigma E_{int}(X_i)$	−509.8	−532.9	−529.2	−514.2	−502.3	−549.4
		E_{int}(est)	−526.5	−528.8	−532.4	−522.7	−505.6	−532.5
		ΔE(calcd−est)	23.2	19.1	26.6	19.4	18.5	21.2
	H_2S, OH^-, H_2CO, $HCOO^-$	E_{int}(calcd)	−464.8	−468.1	−461.4	−454.3	−442.2	−450.8
		$\Sigma E_{int}(X_i)$	−476.9	−485.5	−489.6	−475.7	−460.3	−489.5
		E_{int}(est)	−473.1	−477.2	−477.6	−469.2	−455.6	−474.8
		ΔE(calcd−est)	8.3	9.1	16.2	14.9	13.4	24.0
OH	H_2S, NH_3, Imi, OH^-, SH^-, HCHO	E_{int}(calcd)	−405.5	−403.3	−429.0	−404.8	−401.2	−432.1
		$\Sigma E_{int}(X_i)$	−421.8	−439.2	−479.2	−428.3	−428.4	−480.1
		E_{int}(est)	−404.9	−403.8	−424.3	−406.9	−402.2	−435.7
		ΔE(calcd−est)	−0.6	0.5	−4.7	2.1	1.0	3.6

[a] Sums of interaction energies of ligands with TM Ions, $\Sigma E_{int}(X_i)$ are listed as well (all values in kcal mol^{-1}). [b] CG = coordination geometry, TH = tetrahedral, SQ = square planar, OH = octahedral

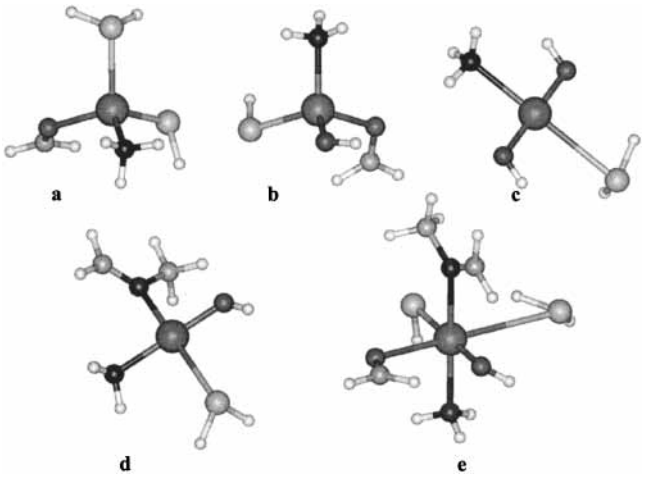

Figure 3. Optimized structures of five persubstituted complexes: **(a)** $[Zn(HCHO)(NH_3)(SH)(H_2S)]^+$, **(b)** $[Zn(HCHO)(NH_3)(OH)(SH)]$ in tetrahedral, **(c)** $[Zn(H_2S)(NH_3)(OH)(OH)]$, **(d)** $[Zn(H_2S)(NH_3)(CH_2NCH_3)(OH)]^+$ in square-planar, **(e)** $[Zn(OH)(SH)(H_2S)(HCHO)(NH_3)(CH_3NCH_2)]$ in octahedral coordination geometry.

values corresponding to a particular coordination geometry) were fully optimized. The complexes are depicted in Figures 3a−e and 4c and e.

The computed interaction energies were then compared to their estimated counterparts, E_{int}(est), calculated according to the equation

$$E_{int}(M, X_1,..., X_n, est) = \sum_i E_{int}(M, X_i) + \frac{1}{2}\sum_{i<j} \Delta E_{coop}(M, X_i, X_j). \quad (3)$$

It should be mentioned that there is no rigorous explanation for the factor of $^1/_2$ in eq 3. It simply determines the weight with which the cooperative effect is included in the calculation of E_{int}(M, X_1,..., X_n, est). The factor $^1/_2$ has been found to yield the best estimates of E_{int}(M, X_1,..., X_n) and probably effectively incorporates the role of higher contributions (many-body interaction terms that can be obtained from tri-, tetra-, etc. substituted complexes, if it were possible to perform these calculations).

The results of the calculations are summarized in Table 4.

In octahedral coordination geometry, the difference between E_{int}(est) and E_{int}(calcd) ranges from −4.7 to 3.6 kcal mol^{-1}. In tetrahedral and square-planar coordination geometries, the values of E_{int}(est) are systematically shifted with respect to those of E_{int}(calcd). Because we are primarily interested in the relative values of E_{int}(M, X_1,..., X_n), the difference between the maximum and minimum of ΔE(calcd-est) for a given system is the most important gauge of the quality of the presumed hypothesis. The values of $\sigma_{calc-est} = |\min_M[\Delta E(\text{calcd-est})] - \max_M[\Delta E(\text{calcd-est})]|$ are 9.9, 13.9, 9.7 (tetrahedral systems), 4.3, 8.1, 15.7 (square-planar systems), and 8.3 kcal mol^{-1} (octahedral system) and can be considered to be the measure of the accuracy of the estimated values of E_{int}(M, X_1,..., X_n). Because the seven model complexes contain one or two anionic ligands and a large cooperative effect is expected (*see* discussion above), we presume that they belong to the systems for which it is more difficult to estimate the values of E_{int}(M, X_1,..., X_n). For this reason, we consider the agreement between the calculated and estimated values of complexation energies to be satisfying and presume that the above values of $\sigma_{calc-est}$ would be at the upper limit of the difference between ΔE(calcd) and ΔE(est). Moreover, slightly higher values of $\sigma_{calc-est}$ calculated for tetrahedral coordination geometry are caused by mercury(II) complexes that are shifted by 6−8 kcal mol^{-1} with respect

TABLE 5: Comparison of Calculated Interaction Energies, $E_{int}(M, X_1,..., X_n)$, Defined by Equation 1 for Small (S) and Large (L) Representations of Three Metal-Binding Sites: [M(Lys)(Cys$^-$)]$^+$ in Linear, [M(His)(Ser)(OH)(Cys$^-$)] in Tetrahedral, and [M(Met)(Ser$^-$)(Asn)(Asp$^-$)] in Square-Planar Coordination Geometry[a]

ligands		Co^{2+}	Ni^{2+}	Cu^{2+}	Zn^{2+}	Cd^{2+}	Hg^{2+}
L: Lys, Cys^-	E_{int}(L)	−326.3	−331.7	−364.0	−320.7	−310.5	−336.8
S: NH_3, SH^-	E_{int}(S)	−306.9	−310.6	−340.6	−302.4	−293.7	−317.4
	E_{int}(L)/E_{int}(S)	1.063	1.068	1.069	1.061	1.057	1.061
	1.063E_{int}(S)	−326.2	−330.2	−362.1	−321.5	−312.2	−337.4
	E_{int}(L) − 1.063E_{int}(S)	−0.1	−1.5	−1.9	0.8	1.7	0.6
L: His, Ser, OH^-, Cys^-	E_{int}(L)	−478.0	−484.8	−497.3	−473.6	−463.5	−481.8
S: Imi, H_2O, OH^-, SH^-	E_{int}(S)	−470.0	−477.9	−490.5	−466.5	−458.4	−475.9
	E_{int}(L)/E_{int}(S)	1.017	1.014	1.014	1.015	1.011	1.012
	1.014E_{int}(S)	−476.6	−484.6	−497.4	−473.0	−464.8	−482.6
	E_{int}(L)−1.014*E_{int}(S)	−1.4	−0.2	0.1	−0.6	1.3	0.8
L: Met, Ser^-, Asn, Asp^-	E_{int}(L)	−474.4	−476.6	−472.3	−462.3	−445.2	−454.8
S: H_2S, OH^-, H_2CO, $HCOO^-$	E_{int}(S)	−464.8	−466.8	−461.4	−454.3	−442.2	−450.8
	E_{int}(L)/E_{int}(S)	1.021	1.021	1.024	1.018	1.007	1.009
	1.016*E_{int}(S)	−472.4	−474.5	−469.0	−461.8	−449.5	−458.2
	E_{int}(L)−1.016*E_{int}(S)	−2.0	−2.1	−3.3	−0.5	4.3	3.4

[a] All values are in kcal mol^{-1}.

to the the values of the other five TM ions, which we point out because at least in the first stage, this fact can be introduced empirically into the calculations of $E_{int}(Hg, X_1,..., X_n)$ for tetrahedral coordination. As has been mentioned above, if all of the ligands in the persubstituted site were neutral and the coordination number was at least 4, the complexation energies could be approximated by the sum of the interaction energies of the individual ligands. However, as can be seen in Table 4, this is not the case for the complexes with anionic ligands, and the explicit consideration of the cooperative effect significantly improves the estimated values in comparison with the $\Sigma E_{int}(X_i)$ terms (two-body interaction terms).

Let us briefly summarize the previous paragraphs. We have shown that the interaction energies of the TM ions with X_n sites that are preorganized into certain coordination geometry (X_is belong to the set of seven simple ligands used for the evaluation of the cooperative effect) can be estimated from knowledge of the interaction energies of individual functional groups with TM ions, $E_{int}(M, X)$, and of the cooperative effect, $\Delta E_{coop}(M, X_i, X_j)$ with reasonable accuracy if the relative scale is applied.

In the second step, the correspondence between the interaction energies calculated for two representations of metal-binding sites is studied. In the first (small) representation, the AA side chains are represented by simple ligands from the set of seven functional groups, whereas in the second (large) representation, whole AA side chains (capped by hydrogens) are used. For example, the side chain of Met is depicted by H_2S in the small representation and by $CH_3CH_2SCH_3$ in the large representation. Three pairs of corresponding model systems are $[M(NH_3)(SH)]^+$ and [M(Lys)(Cys$^-$)]$^+$ in linear (denoted as pair 1 and depicted in Figure 4a and b), $[M(CH_3NCH_2)(H_2O)(OH)(SH)]$ and [M(His)(Ser)(OH)(Cys$^-$)] in tetrahedral (pair 2, Figure 4c and d), and $[M(H_2S)(OH)\ (H_2CO)(HCOO)]$ and [M(Met)(Ser$^-$)-(Asn)(Asp$^-$)] in square-planar coordination geometry (pair 3, Figure 4e and f).

The same computational scheme as that used in the previous step has been adopted (i.e., full optimizations for all systems, with only the angles at the metal center fixed at the particular coordination geometry). The only exceptions were linear systems, $[M(NH_3)(SH)]^+$, [M(Lys)(Cys$^-$)]$^+$, where the angles S−M−N at the metal center (180°) have been optimized, as well. The resulting structures only slightly deviate from linear coordination geometry (S−M−N = 173−177°). The calculated interaction energies for all systems are listed in Table 5.

As anticipated, the values of E_{int}(L) and E_{int}(S) differ, but

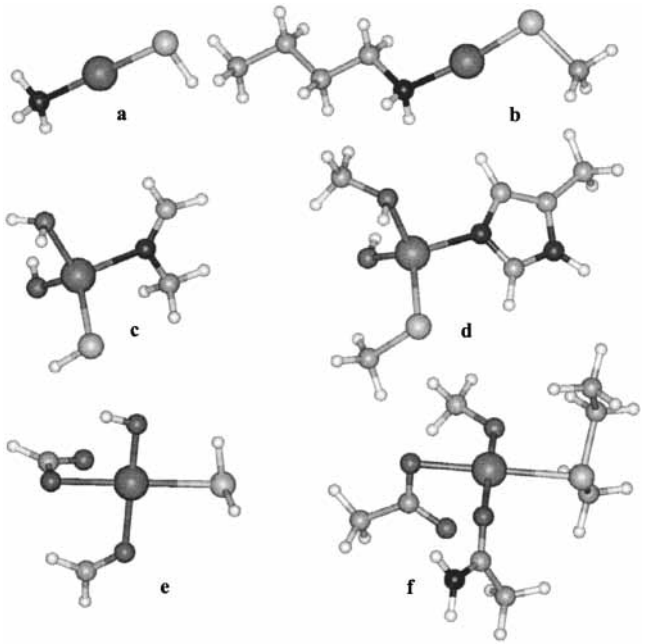

Figure 4. Three pairs of corresponding model systems used for the comparison of small and large representations of metal-binding sites in metalloproteins: **(a)** $[M(NH_3)(SH)]^+$ and **(b)** [M(Lys)(Cys$^-$)]$^+$ in linear, **(c)** $[M(CH_3NCH_2)(H_2O)(OH)(SH)]$ and **(d)** [M(His)(Ser)(OH)-(Cys$^-$)] in tetrahedral, **(e)** $[M(H_2S)(OH)(H_2CO)(HCOO)]$ and **(f)** [M(Met)(Ser$^-$)(Asn)(Asp$^-$)] in square-planar coordination geometry.

the important observation is that their ratios remain almost constant over the six TM ions (1.057−1.069 for pair 1 in linear, 1.011−1.017 for pair 2 in tetrahedral, and 1.007−1.024 for pair 3 in square-planar coordination geometry). If E_{int}(S) is scaled by the average of E_{int}(L)/E_{int}(S), we obtain values that differ by −1.9 to 1.7 (Lin), −1.4 to 1.3 (TH), and −3.3 to 4.3 (SQ) kcal mol^{-1} from the computed values of E_{int}(L). Therefore, a very nice linear relationship between the two representations has been established (for Cd^{2+} and Hg^{2+} in square-planar geometry, namely, the [M(Met)(Ser$^-$)(Asn)(Asp$^-$)] complex and the corresponding small representation, the agreement is slightly worse (see the last row of Table 5), which might be caused by the more complicated binding modes of carboxylate residues).[31]

What are the consequences of this finding? Let us suppose that the target structure is a real metal-binding site in a metalloprotein in a given coordination geometry. The specificity of a given site is determined by the differences in the stability

constants of individual TM ions (i.e., by ΔG^0 for the process of desolvation of the TM ion, its subsequent in vacuo complexation in the metal-binding site, and solvation of the entire [metal−biomolecule] complex ($\Delta G^0 = \Delta G^0_{desolv} + \Delta G^0_{int} + \Delta G^0_{solv}$)). ΔG^0_{desolv} is the quantity inherent to each TM ion and is independent of the particular site. On the other hand, ΔG^0_{solv} of the entire complex can be considered to be constant (for the given site) in series of TM ions with the same charge and coordination number. Therefore, if we are interested in the relative specificities (i.e., the differences in the binding of individual TM ions in the particular site), ΔG^0 could be reasonably approximated by ΔG^0_{int}. Furthermore, if the entropy contributions are considered constant, which is a plausible approximation, and if the above conditions are fulfilled, then ΔG^0_{int} is equal (allowing for a constant) to ΔE^0_{int}, the in vacuo complexation energy of the TM ion in the site. The comparison of small and large representations demonstrates that for the given site $E_{int}(M, X_1,..., X_n)$ can have a linear relationship with ΔE^0_{int}, a value unattainable by any experiment or quantum chemical calculations. This presumption has been ascertained to the level of representing the metal-binding site in a protein with full AA side chains. Taking into account all these considerations, the effects of the environment (solvation, protein bulk) on the values of the relative affinities are negligible. On an absolute scale, which is especially applicable to anionic ligands, ΔG^0 will significantly differ from ΔE^0_{int}, but they will be in a linear relationship for the series of TM ions discussed in this article (although coefficients may differ from site to site).

Moreover, it has been demonstrated that the estimates of $E_{int}(M, X_1,..., X_n)$ for small representations can be calculated to good accuracy from the values of the interaction energies of individual functional groups with TM ions and quantitative knowledge of the cooperative effect, thus a large number of metal-binding sites can be readily scanned for their selectivity toward the six TM ions from our data.

It should be noted that we have also tested the second alternative route to accurate estimates of $E_{int}(M,Y_1,...,Y_n)$. The values of $E_{int}(M,Y_1,...,Y_n, est)$ are calculated according to the equation

$$E_{int}(M, Y_1,..., Y_n, est) = \sum_i E_{int}(M, Y_i) + f \sum_{i<j} p_{coop}(M, X_i, X_j)(|E_{int}(M, Y_i)| + |E_{int}(M, Y_j)|), \quad (4)$$

where $f = 1$ for linear and $^1/_2$ for other coordination geometries (see the discussion above), Y_i's are whole amino acid side chains, and X_i's are the corresponding functional groups from the small representations (e.g., H_2S for Met, HCHO for Asn and Gln, etc.). In this way, it is assumed that the cooperative effect is (on a relative scale) equivalent for small and large representations of amino acid side chains. However, this approach has yielded worse results than the above- described strategy. We can think of two reasons. First, when using a small representation, all the ligands (including nonsubstituted water molecules) are approximately the same size, and the complex, as the model of a more complex metal-binding site, is well-balanced. On the other hand, when we use the interaction energies of whole amino acid side chains, $E_{int}(M,Y)$, acquired from the calculations of $[M(H_2O)_{n-1}Y]^{2+}$ complexes, they may be exaggerated for large functional groups such as Lys and Tyr (induction effect of alkyl or aryl groups) because the remaining $n - 1$ water molecules are small ligands and the complex is not well-balanced on the side of the ligands. Then, the cooperative effect, calculated for a small representation, does not improve the deficiency, even if the relative values of $p_{coop}(M, X_i, X_j)$ are applied. The second problem with this strategy stems from the propagation of computational errors that are present in each value of $E_{int}(M,Y)$ and $E_{int}(M, X,Y)$. If the calculated value of the denominator in eq 2a, $|E_{int}(M, X_i)| + |E_{int}(M, X_j)|$, is close to zero, then $p_{coop}(M, X_i, X_j)$ can be quite large, owing to the inherent computational error (1−2 kcal mol^{-1}) in each of the calculated values. Then, if ($|E_{int}(M,Y_i)| + |E_{int}(M,Y_j)|$) for a large representation (whole AA side chains) differs from zero, the error in the estimated $\Delta E_{coop}(M,Y_i,Y_j)$ value can be enormous.

Because we consider the agreement between the estimated and calculated values of complexation energies and the correspondence between the small and large representations of a particular metal-binding site to be the most important findings of this work, the whole procedure for estimating the complexation energies of the ions in general metal-binding sites will be briefly recounted:

(i) Represent a metal-binding site in a metalloprotein by a complex $[MX_n]^{2+}$, where all the X_i's belong to the set of seven simple functional groups (OH^-, H_2S, SH^-, HCHO, $HCOO^-$, NH_3, and CH_3NCH_2), and assign the target coordination geometry.

(ii) From the data in Table 1, calculate the sum of the interaction energies, $\Sigma E_{int}(X_i)$, for all ligands (for R−OH residues, represented by H_2O, the interaction energy is zero).

(iii) For all pairs of the participating functional groups, calculate the sum of the energies quantifying a cooperative effect, $\Delta E_{coop}(M, X, Y)$. These values are to be found in Table 2. Add this value of ΔE_{coop}, multiplied by the factor $f = 1$ (linear) or $^1/_2$ (tetrahedral, square-planar, and octahedral coordination geometries) to $\Sigma E_{int}(X_i)$ calculated in (ii), and obtain the estimates of the complexation energies of TM ions in this site with a relative accuracy 5−15 kcal mol^{-1}, which is the average error bar that has been found for seven model systems computed in this work.

(iv) For further refinement of these values, data listed in Tables 2−5 in the preceding article[18] can be used. These Tables contain the interaction energies of the whole AA side chains with the TM ions and yield information that may be used to discern small differences in the binding of AA residues represented by the same simple functional groups (e.g., His bound by Nδ and Nϵ, Asp vs Glu, or AA side chains containing a hydroxyl group (Ser, Thr, Tyr)).

Comparison of the Complexation Energies of the TM Ions with the Stability Constants in the Metal-Binding Sites of Metalloproteins. To ascertain the credibility of the computed data and further verify the above hypothesis about the linear relationship between ΔE^0_{int} and ΔG^0, we correlated the estimated or calculated complexation energies with experimentally determined stability constants of TM ions in metal-binding sites of metalloproteins. The relevant experimental data can be found for carbonic anhydrase (CA)[32] and carboxypeptidase A (CPDA).[33] Because the stability constants were measured in aqueous solution, the reference state for each metal ion is its hexahydrate complex, $[M(H_2O)_6]^{2+}$. The hypothetical process of the complexation of a particular TM ion in an (X_n) site is then (schematically)

$$[M(H_2O)_6]^{2+} \xrightarrow{\Delta E_1} [M(H_2O)_n]^{2+} + (6 - n)H_2O$$

$$[M(H_2O)_n]^{2+} + nX - nH_2O \xrightarrow{\Delta E_2} [MX_n]^{2+}$$

The values of ΔE_1 can be found in Table 1 in the preceding article of the series ($E_{OH}(M) - E_{Gm}(M)$),[18] whereas ΔE_2 is the

TABLE 6: Comparison of the Estimated (Calculated) Complexation Energies with the Stability Constants for Metal-Binding Sites of Two Metalloproteins—Carbonic Anhydrase and Carboxypeptidase

	carbonic anhydrase		carboxypeptidase A	
TM ion	ΔE (kcal mol^{-1})	K_{exp}[a]	ΔE (kcal mol^{-1})	K_{exp}[b]
Co^{2+}	−248.3	7.2	−123.8	7.7
Ni^{2+}	−237.3	9.5	−124.7	9.9
Cu^{2+}	−258.1	11.6		
Zn^{2+}	−248.9	10.5	−139.1	10.2
Cd^{2+}	−237.1	9.2	−147.9	11.0
Hg^{2+}	−260.3	21.5	−192.0	22.0

[a] Ref 32. [b] Ref 33 (the values for cupric complexes are not available).

interaction (complexation) energy $E_{int}(M, X_1,..., X_n)$ whose calculation or estimation is the central subject of this work. The straightforward application of this scheme to the tetrahedral (His, His, His, OH^-) site in CA (with ΔE_2 estimated) and the linear (His, SH^-) site of CPDA (with ΔE_2 calculated) leads to the results summarized in Table 6 ($\Delta E = \Delta E_1 + \Delta E_2$).

It can be seen that the experimentally determined order in stability constants ($Hg^{2+} \gg Cu^{2+} > Zn^{2+} > Cd^{2+}$, $Ni^{2+} > Co^{2+}$ for CA; $Hg^{2+} \gg Cd^{2+} > Zn^{2+} > Ni^{2+} > Co^{2+}$ for CPDA) is qualitatively well-reproduced by theory ($Hg^{2+} > Cu^{2+} > Zn^{2+} > Co^{2+} > Cd^{2+}$, Ni^{2+} for CA; $Hg^{2+} \gg Cd^{2+} > Zn^{2+} > Ni^{2+} > Co^{2+}$ for CPDA), with only one exception of a Co^{2+} ion in the CA site whose complexation energy is slightly (∼8 kcal mol^{-1}) overestimated. Quite remarkably (considering the simplicity of the model system), even the equal stability of Ni^{2+} and Cd^{2+} in the metal-binding site of carbonic anhydrase is reproduced. We would like to use these results as supporting evidence for our hypothesis that the complexation energies of a series of TM ions with the same charge are, to a great extent, determined by the structure of the first coordination sphere and to demonstrate that data published in this article can provide the entire community of bioinorganic chemists with rough estimates of the relative order of stability constants of the TM ions in mononuclear metal-binding sites of metalloproteins.

IV. Conclusions

(i) The cooperative effect accompanying the simultaneous substitution of two functional groups for water molecules in reference perhydrated $[M(H_2O)_n]^{2+}$ complexes and the nonadditivity in corresponding physical quantities, namely, the interaction energies, have been quantitatively evaluated. This effect is often mentioned as playing a nonmarginal role in many chemically important systems (not only TM complexes), but to our knowledge, we present the first systematic study that considers a large series of TM ions and biologically relevant ligands. The effect is fairly small (less than 2 kcal mol^{-1}) for neutral ligands and coordination geometries other than linear, which means that the complexation energies of TM ions in neutral metal-binding sites can be estimated from the published interaction energies of individual AA side chains with TM ions. However, the effect is of a nonnegligible magnitude for negatively charged ligands and linear coordination geometry, which has been explained by the effective strength of the interaction between TM ions and ligands. This finding implies that the usage of force-field approaches (including, in most of their functional form, only two-body nonbond interaction terms) for studies of the energetics of TM systems is erroneous.

(ii) The stabilities of cis and trans isomers of complexes in square-planar and octahedral coordination geometries have been calculated, and the observed trends have been explained on the basis of the changes in electron distribution accompanying charge transfer from ligands to a metal ion. This finding is noteworthy because the higher stability of the trans isomers of the complexes containing anionic ligands is often explained purely on the basis of the electrostatic repulsion of the ligands. We have shown that it is the above-described charge transfer that is the basis of this phenomenon. This part of our work can be pursued further and analyzed in more detail, but because it is not the main focus of this article, we have restricted it to only three representative pairs of complexes.

(iii) It has been shown that the complexation energies of TM ions in a persubstituted metal-binding site of a general formula $[MX_n]^{2+}$ (X_i's are simple ligands representing AA side chains $-OH^-$, H_2S, SH^-, HCHO, $HCOO^-$, NH_3, CH_3NCH_2) can be estimated to a good accuracy from the interaction energies of these functional groups and the quantitative knowledge of cooperative effect.

(iv) Very good correspondence between small (vide supra) and large (X_i's are whole AA side chains) representations of metal-binding sites has been established, which implies that a very large number of mononuclear metal-binding sites containing TM ions can be readily scanned for their selectivity toward these ions from the computed data.

(v) Good correlation between the complexation energies of TM ions in metal-binding sites of carbonic anhydrase and carboxypeptidase A and the experimentally determined stability constants of TM ions in these sites has been found, which implies that metal ion selectivity is determined, to a great extent, by the local structure and energetics of the particular metal site.

The advantage of the adopted model is that a very large number of systems have been studied, and their interaction energies have been compared. This model enabled us to calculate the energy-derived properties on a relative scale and also resulted in the cancellation of errors in the computational procedures. We believe that only in this way can many principal obstacles (e.g., different relative permittivities in vacuo, in biomolecules, and in water solutions, which makes the direct extrapolation of ab inito results to realistic chemical systems at least questionable) be eliminated.

On the other hand, it must be stressed that the model is limited to mononuclear metal-binding sites in biomolecules because the structures of polynuclear TM systems are determined to a large extent by the character of metal−metal bonds. Furthermore, the model does not consider any steric restrictions upon the side of ligands (e.g., the fact that AA side chains binding to TM ions in metalloproteins are linked by a polypeptide chain). However, it has been shown by quantum chemical calculations that this so-called entatic effect is not so important for the chemical and physical properties of metal-binding sites[1e,2e] ; therefore, we believe that our conclusions (metal ion selectivities) can be transferred to a metalloprotein sites without a great loss of accuracy.

Acknowledgment. This work was supported by projects LN00A032 (Center for Complex Molecular Systems and Biomolecules) and Z4055905 and grants 203/01/0832 (GA CR) and A4055103/01 (GA AV CR). CPU time on Origin 2000 at MU Brno (project MetaCentre) and NEC-SX4 at CHMI (grant no. LB98202, project INFRA2 of MSMT CR) is gratefully acknowledged. We also thank one of the referees who brought to our attention two experimental papers dealing with the stability constants of carbonic anhydrase and carboxypeptidase A.

Supporting Information Available: The geometries of all the complexes (1236 systems) optimized according to the

described procedures at the B3LYP/BS1 level and their molecular energies in hartrees computed at the B3LYP/BS2 level (for both $[MX_n]^{2+}$ and $[Bq_MX_n]^{2+}$ systems). This material is available via the Internet at http://pubs.acs.org.

References and Notes

(1) (a) Garmer, D. R.; Krauss, M. *J. Am. Chem. Soc.* **1992**, *114*, 6487. (b) Ghosh, P.; Shabat, D.; Kumar, S.; Sinha, S. C.; Grynszpan, F.; Li, J.; Noodleman, L.; Keinan, E. *Nature* **1996**, *382*, 339. (c) Zwaans, R.; van Lenthe, J. H.; den Boer, D. H. W. *J. Mol. Struct.* **1996**, *367*, 15. (d) Ryde, U.; Hemmingsen, L. *J. Biol. Inorg. Chem.* **1997**, *2*, 567. (e) Pierloot, K.; De Kerpel, J. O. A.; Ryde, U.; Olsson, M. H. M.; Roos B. O. *J. Am. Chem. Soc.* **1998**, *120*, 13156. (f) De Kerpel, J. O. A.; Pierloot, K.; Ryde, U. *J. Phys. Chem. B* **1999**, *103*, 8375. (g) Noy, D.; Yerushalmi, R.; Brumfeld, V.; Ashur, I.; Scheer, H.; Baldridge, K. K.; Scherz, A. *J. Am. Chem. Soc.* **2000**, *122*, 3937.

(2) (a) Glusker, J. P. *Adv. Protein Chem.* **1991**, *42*, 1. (b) Šponer, J.; Sabat, M.; Burda, J. V.; Leszczynski, J.; Hobza, P. *J. Phys. Chem. B* **1999**, *103*, 2528. (c) Šponer, J.; Šponer, J. E.; Gorb, L.; Leszczynski, J.; Lippert, B. *J. Phys. Chem. A* **1999**, *103*, 11406. (d) Šponer, J.; Sabat, M.; Gorb, L.; Leszczynski, J.; Lippert, B.; Hobza, P. *J. Phys. Chem. B* **2000**, *104*, 7535. (e) Ryde, U.; Olsson, M. H. M. *Int. J. Quantum Chem.* **2001**, *81*, 335.

(3) (a) Siegbahn, P. E. M.; Eriksson, L.; Himo, F.; Pavlov, M. *J. Phys. Chem. B* **1998**, *102*, 10622. (b) Siegbahn, P. E. M.; Crabtree, R. H. *J. Am. Chem. Soc.* **1999**, *121*, 117. (c) Siegbahn, P. E. M. *Inorg. Chem.* **2000**, *39*, 2923. (d) Li, J.; Nelson, M. R.; Peng, C. Y.; Bashford, D.; Noodleman, L. *J. Phys. Chem. A* **1998**, *102*, 6311. (e) Li, J.; Fisher, C. L.; Konecny, R.; Bashford, D.; Noodleman, L. *Inorg. Chem.* **1999**, *38*, 929. (f) Konecny, R.; Li, J.; Fisher, C. L.; Dillet, V.; Bashford, D.; Noodleman, L. *Inorg. Chem.* **1999**, *38*, 940. (g) Himo, F.; Eriksson, L. A.; Maseras, F.; Siegbahn, P. E. M. *J. Am. Chem. Soc.* **2000**, *122*, 8031. (h) Siegbahn, P. E. M. *J. Biol. Inorg. Chem.* **2001**, *6*, 27.

(4) (a) Broclawik, E.; Salahub, D. R. *J. Mol. Catal.* **1993**, *82*, 117. (b) Deeth, R. J. *J. Chem. Soc., Faraday Trans.* **1993**, *89*, 3745. (c) Åkesson, R.; Pettersson, L. G. M.; Sandström, M.; Wahlgren, U. *J. Am. Chem. Soc.* **1994**, *116*, 8691. (d) Åkesson, R.; Pettersson, L. G. M.; Sandström, M.; Wahlgren, U. *J. Am. Chem. Soc.* **1994**, *116*, 8705. (e) Fournier, R. *Theor. Chim. Acta* **1995**, *91*, 129. (f) Fournier, R. *J. Chem. Phys.* **1995**, *102*, 5396. (g) Li, J.; Fisher, C. L.; Chen, J. L.; Bashford, D.; Noodleman, L. *Inorg. Chem.* **1996**, *35*, 4694. (h) Bray, M. R.; Deeth, R. J.; Paget, V. J.; Sheen, P. D. *Int. J. Quantum Chem.* **1996**, *61*, 85. (i) Adamo, C.; Lelj, F. *J. Mol. Struct.* **1997**, *389*, 83. (j) Niu, S.; Hall, M. B. *J. Phys. Chem A* **1997**, *101*, 1360. (k) Thomas, J. L. C.; Bauschlicher, C. W., Jr.; Hall, M. B. *J. Phys. Chem A* **1997**, *101*, 8530. (l) Barone, V.; Adamo, C. *Int. J. Quantum Chem.* **1997**, *61*, 443. (m) Irigoras, A.; Fowler, J. E.; Ugalde, J. M. *J. Am. Chem. Soc.* **1999**, *121*, 8549. (n) Hoyau, S.; Ohanessian, G. *J. Am. Chem. Soc.* **1997**, *119*, 2016. (o) Schröder, D.; Schwarz, H.; Hrušák, J.; Pyykkö, P. *Inorg. Chem.* **1998**, *37*, 624. (p) Bärsch, S.; Schröder, D.; Schwarz, H. *Helv. Chim. Acta* **2000**, *83*, 827. (q) Kretzschmar, I.; Schröder, D.; Schwarz, H.; Rue, C.; Armentrout, P. B. *J. Phys. Chem. A* **2000**, *104*, 5046. (r) Rogalewicz, F.; Hoppilliard, Y.; Ohanessian, G. *Int. J. Mass. Spectrom.* **2001**, *206*, 45.

(5) (a) Niu, S.; Hall, M. B. *Chem. Rev.* **2000**, *100*, 353. (b) Loew, G. H.; Harris, D. L. *Chem. Rev.* **2000**, *100*, 407. (c) Siegbahn, P. E. M.; Blomberg, M. R. A. *Chem. Rev.* **2000**, *100*, 421. (d) Frenking, G.; Fröhlich, N. *Chem. Rev.* **2000**, *100*, 717. (e) Hush, N. S.; Reimers, J. R. *Chem. Rev.* **2000**, *100*, 775.

(6) Siegbahn, P. E. M.; Blomberg, M. R. A. *Annu. Rev. Phys. Chem.* **1999**, *50*, 221.

(7) Papai, I. *J. Chem. Phys.* **1995**, *103*, 1860.

(8) Taketsugu, T.; Gordon, M. S. *J. Chem. Phys.* **1997**, *106*, 8504.

(9) de Bruin, T. J. M.; Marcelis, A. T. M.; Zuilhof, H.; Sudholter, E. J. R. *Phys. Chem. Chem. Phys.* **1999**, *1*, 4157.

(10) Bluhm, B. K.; Shields, S. J., Bayse C. A.; Hall, M. B.; Russell, D. H. *Int. J. Mass. Spectrom.* **2001**, *204*, 31.

(11) Bertini, I.; Briganti, F.; Scozzafava, A. In *Handbook of Metal−Ligand Interactions in Biological Fluids*; Berthon, G., Ed.; Marcel Dekker: New York, 1995; pp 81−91.

(12) Rulíšek, L.; Vondrášek, J. *J. Inorg. Biochem.* **1998**, *71*, 115.

(13) Cotton, F. A.; Wilkinson, G. *Advanced Inorganic Chemistry*, 4th ed.; Wiley & Sons: NewYork, 1980.

(14) (a) Pearson, R. G. *J. Am. Chem. Soc.* **1963**, *85*, 3533. (b) Parr, R. G.; Pearson, R. G. *J. Am. Chem. Soc.* **1983**, *105*, 7512.

(15) (a) Sigel, H.; McCormick, D. B. *Acc. Chem. Res.* **1970**, *3*, 201. (b) Martin, R. B. *J. Chem. Educ.* **1987**, *64*, 402.

(16) Rulíšek, L.; Havlas, Z. *J. Phys. Chem. A* **1999**, *103*, 1634.

(17) Rulíšek, L.; Havlas, Z. *J. Chem. Phys.* **2000**, *112*, 149.

(18) Rulíšek, L.; Havlas, Z. *J. Am. Chem. Soc.* **2000**, *122*, 10428.

(19) In the formulas of complexes with the general ligands (X, Y) such as $[M(H_2O)_{n-2}XY]^{2+}$, we write the total charge of the complex as +2, though we are aware that if X or Y is an anionic ligand, it has smaller value (0, +1). We hope that this idea is quite clear in the context of this work.

(20) The cations of Mn and Fe would probably make the set of TM ions more complete. One of the reasons that they were not included in the study is that most of their metal binding sites are not mononuclear (see, for example, ref 5c) and many of them possess quite unique features that prevent them from being the subject of a similar study.

(21) Fraústo da Silva, J. J. R.; Williams, R. J. P. *The Biological Chemistry of the Elements*; Clarendon: Oxford, U. K., 1991.

(22) (a) Sousa, C.; Cebolla, A.; de Lorenzo, V. *Nature Biotechnol*. **1996**, *14*, 1017. (b) Brown, S. *Nature Biotechnol.* **1997**, *15*, 269. (c) Dahiyat, B. I.; Mayo, S. L. *Science* **1997**, *278*, 82. (d) DeGrado, W. F.; Summa, C. M.; Pavone, V.; Nastri, F.; Lombardi, A. *Annu. Rev. Biochem.* **1999**, *68*, 779. (e) Kostal, J.; Mulchandani, A.; Chem, W. *Macromolecules* **2001**, *34*, 2257.

(23) Frisch, M. J.; Trucks, G. W.; Schlegel, H. B.; Scuseria, G. E.; Robb, M. A.; Cheeseman, J. R.; Zakrzewski, V. G.; Montgomery, J. A., Jr.; Stratmann, R. E.; Burant, J. C.; Dapprich, S.; Millam, J. M.; Daniels, A. D.; Kudin, K. N.; Strain, M. C.; Farkas, O.; Tomasi, J.; Barone, V.; Cossi, M.; Cammi, R.; Mennucci, B.; Pomelli, C.; Adamo, C.; Clifford, S.; Ochterski, J.; Petersson, G. A.; Ayala, P. Y.; Cui, Q.; Morokuma, K.; Malick, D. K.; Rabuck, A. D.; Raghavachari, K.; Foresman, J. B.; Cioslowski, J.; Ortiz, J. V.; Stefanov, B. B.; Liu, G.; Liashenko, A.; Piskorz, P.; Komaromi, I.; Gomperts, R.; Martin, R. L.; Fox, D. J.; Keith, T.; Al-Laham, M. A.; Peng, C. Y.; Nanayakkara, A.; Gonzalez, C.; Challacombe, M.; Gill, P. M. W.; Johnson, B. G.; Chen, W.; Wong, M. W.; Andres, J. L.; Head-Gordon, M.; Replogle, E. S.; Pople, J. A. *Gaussian 98*, revision A.6; Gaussian, Inc.: Pittsburgh, PA, 1998.

(24) Becke, A. D. *J. Chem. Phys.* **1993**, *98*, 5648.

(25) (a) Becke, A. D. *Phys. Rev. A: At., Mol., Opt. Phys.* **1988**, *38*, 3098. (b) Lee, C.; Yang, W.; Parr, R. G. *Phys. Rev. B: Condens. Matter* **1988**, *37*, 785. (c) Vosko, S. H.; Wilk, L.; Nusair, M. *Can. J. Phys.* **1980**, *58*, 1200.

(26) (a) Watchers, A. J. H. *J. Chem. Phys.* **1970**, *52*, 1033. (b) Hay, P. J. *J. Chem. Phys.* **1977**, *66*, 4377. (c) Raghavachari, K.; Trucks, G. W. *J. Chem. Phys.* **1989**, *91*, 1062.

(27) (a) McLean, A. D.; Chandler, G. S. *J. Chem. Phys.* **1980**, *72*, 5639. (b) Krishnan, R.; Binkley, J. S.; Seeger, R.; Pople, J. A. *J. Chem. Phys.* **1980**, *72*, 650.

(28) Stevens, W. J.; Krauss, M.; Basch, H.; Jasien, P. G. *Can. J. Chem.* **1992**, *70*, 612.

(29) Marcus, Y. *Chem. Rev.* **1988**, *88*, 1475.

(30) Blomberg, M. R. A.; Siegbahn, P. E. M. *Theor. Chem. Acc.* **1997**, *97*, 72.

(31) Ryde, U. *Biophys. J.* **1999**, *77*, 2777.

(32) Lindskog, S.; Nyman, P. O. *Biochim. Biophys. Acta* **1964**, *85*, 462.

(33) Coleman, J. E.; Vallee, B. L. *J. Biol. Chem.* **1961**, *236*, 2244.